

Hypernuclei and in-medium chiral dynamics

Paolo Finelli^a

Physics Department, University of Bologna,
 Via Irnerio 46, 40126 Bologna (Italy)

Abstract. A recently introduced relativistic nuclear energy density functional, constrained by features of low-energy QCD, is extended to describe the structure of hypernuclei. The density-dependent mean field and the spin-orbit potential of a Λ -hyperon in a nucleus, are consistently calculated using the $SU(3)$ extension of in-medium chiral perturbation theory. The leading long-range ΛN interaction arises from kaon-exchange and 2π -exchange with a Σ -hyperon in the intermediate state. Scalar and vector mean fields, originating from in-medium changes of the quark condensates, produce a sizeable *short-range* spin-orbit interaction. The model, when applied to oxygen as a test case, provides a natural explanation for the smallness of the effective Λ spin-orbit potential: an almost complete cancellation between the background contributions (scalar and vector) and the long-range terms generated by two-pion exchange.

1 Hypernuclear phenomenology

A hypernucleus is a nucleus in which one or more nucleons have been replaced by strange baryons [1,2]. In particular, Λ -hypernuclei are quantum systems composed of a single Λ -hyperon plus a core of nucleons. The standard notation, used throughout this work, is

$${}^A_Z\Lambda \quad \text{where} \quad \begin{cases} A : & \text{total number of baryons (nucleons + hyperon)} \\ Z : & \text{total charge (not necessarily the number of protons)} \\ \Lambda : & \text{hyperon (in this case, but in general, also } \Sigma, \Xi, \dots) \end{cases}$$

For instance, ${}^{13}_{\Lambda}\text{C} = 6p + 6n + \Lambda$. A simple way to describe hypernuclear properties is to employ a phenomenological potential [3]

$$U^{\Lambda}(r) = U_c^{\Lambda}(r) + U_{ls}^{\Lambda}(r), \quad (1)$$

where

$$U_c^{\Lambda}(r) = -V_c^{\Lambda} f(r) \quad \text{and} \quad U_{ls}^{\Lambda} = V_{ls}^{\Lambda} \left(\frac{\hbar}{m_{\pi} c} \right)^2 \frac{1}{r} \frac{df(r)}{dr} \mathbf{s} \cdot \mathbf{l}, \quad (2)$$

are the central and spin-orbit terms, respectively. $f(r)$ is a radial form factor that can be determined from the corresponding nuclear density distribution $f(r) = \rho(r)/\rho(0)$, or chosen in a Woods-Saxon form $f(r) = 1/\{1 + \exp[(r-R)/a]\}$. In Fig. 1 we display the Λ binding energies B_{Λ} for a set of hypernuclei, as functions of $A^{-3/2}$. The dashed curves are extrapolations to the nuclear-matter limit ($A \rightarrow \infty$). When compared to the binding of a nucleon, one notes a considerable reduction of B_{Λ} . The strength of the central potential V_c^{Λ} is estimated [3]¹

^a e-mail: paolo.finelli@bo.infn.it

¹ This analysis is based on data for light and medium hypernuclei (from ${}^{12}_{\Lambda}\text{C}$ to ${}^{40}_{\Lambda}\text{Ca}$), but the inclusion of heavier hypernuclei does not change the estimate of Eq. (3) significantly (28 MeV for a fit with a Woods-Saxon potential [4]).

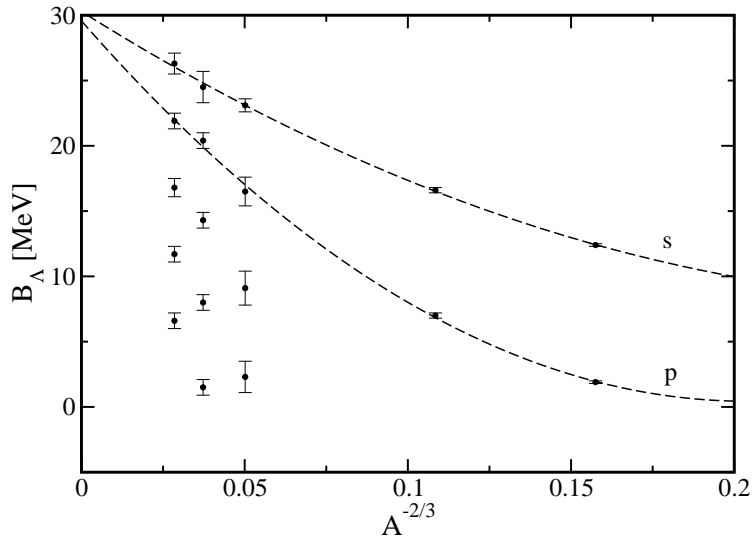


Fig. 1. Data on binding energies B_Λ of Λ single-particle states (in various orbits) as functions of $A^{-2/3}$, where A is the mass number of the nuclear core (see also Ref. [4]). The experimental values have been taken from Ref. [5] (Tables 11 and 13). The dashed curves extrapolate the values of B_Λ to the nuclear-matter limit ($A^{-2/3} \rightarrow 0$).

$$V_c^A \simeq 32 \pm 2 \text{ MeV} , \quad (3)$$

i.e. about 2/3 of the depth of the nucleon potential. On the other hand, the Λ -nucleus spin-orbit interaction is extremely weak [3]:

$$V_{ls}^A \simeq 4 \pm 2 \text{ MeV} . \quad (4)$$

This peculiar property has recently been confirmed by the E929 BNL experiment [6], which observed the spin-orbit splitting between $(p_{1/2})_\Lambda$ and $(p_{3/2})_\Lambda$ orbits in $^{13}_\Lambda\text{C}$, by separately detecting the Λ inter-shell transitions $(p_{1/2})_\Lambda \rightarrow (s_{1/2})_\Lambda$ and $(p_{3/2})_\Lambda \rightarrow (s_{1/2})_\Lambda$ around 11 MeV (see Fig. 2). The observed energy spacing is $E(1/2^-) - E(3/2^-) = 152 \pm 54 \pm 36 \text{ keV}$. Measurements of such high precision are feasible because the spreading widths of the Λ hypernuclear states are extremely small [5].

Considering that the corresponding spin-orbit strength for the nucleon is an order of magnitude larger ($V_{ls}^N \sim 20 \text{ MeV}$), it is extremely important to understand the microscopic mechanism at the basis of this unnatural property.

2 In-medium chiral dynamics applied to hypernuclei

A novel approach to the nuclear many-body problem, based on in-medium chiral effective field theory, has recently been successfully applied to nuclear matter and properties of finite nuclei [7,8,9,10]. In particular, it has been demonstrated that iterated one-pion exchange and irreducible 2π exchange processes, with inclusion of Pauli blocking effects and Δ -isobar excitations in intermediate states, generate the correct nuclear binding [7,8]. The nuclear spin-orbit potential, on the other hand, is produced by the coherent action of scalar and vector mean fields, representing the in-medium changes of the quark condensates [9,10,11,12,13,15]. The importance of correlated 2π exchange for hypernuclei was already pointed out in Ref. [16], and recently the in-medium chiral approach has been extended to include the strangeness degree of freedom [17]. The long-range ΛN interaction arising from kaon and 2π exchange, with a Σ -hyperon and medium insertions in intermediate states, has been explicitly calculated in a

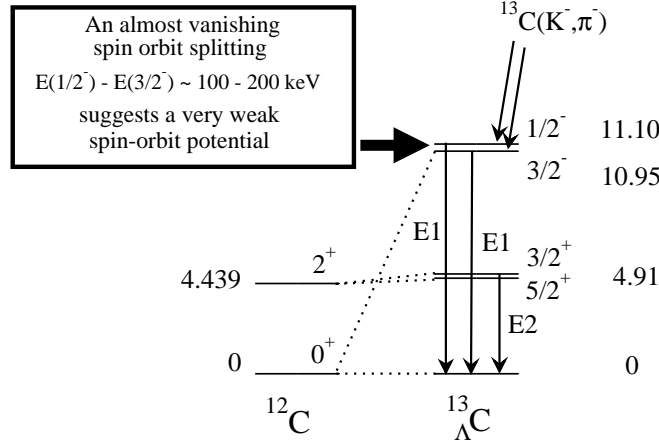


Fig. 2. The hypernuclear γ transitions observed in $^{13}_{\Lambda}\text{C}$ [5,6]. The levels are denoted by their excitation energy (in MeV), and the spin and parity. The observed spin-orbit splitting is small ($154 \pm 54 \pm 36 \text{ keV}$), i.e. $20 \sim 30$ times smaller than that of the nucleon p -levels. The ordering of the Λ p -levels appears to be the same as for the nucleon levels. (From Fig. 47 in Ref. [5]).

controlled expansion in powers of the Fermi momentum k_f . In Ref. [18] this approach has been applied to finite hypernuclei.

2.1 The model

In order to describe hypernuclei we extend the relativistic nuclear energy density functional (see Sec. 2.2 of Ref. [10]), by adding the hyperon contribution:

$$E_0[\rho] = E_0^N[\rho] + E_0^A[\rho], \quad (5)$$

where $E_0^N[\rho]$ describes the core of protons and neutrons (cf. Eq. (12) in Ref. [10]), and $E_0^A[\rho]$ is the leading-order term representing the single Λ -hyperon, decomposed in free and interaction parts:

$$E_0^A[\rho] = E_{\text{free}}^A[\rho] + E_{\text{int}}^A[\rho], \quad (6)$$

with

$$E_{\text{free}}^A = \int d^3r \langle \phi_0 | \bar{\psi}_\Lambda [-i\boldsymbol{\gamma} \cdot \boldsymbol{\nabla} + M_\Lambda] \psi_\Lambda | \phi_0 \rangle \quad (7)$$

$$E_{\text{int}}^A = \int d^3r \left\{ \langle \phi_0 | G_S^A(\rho) (\bar{\psi}\psi) (\bar{\psi}_\Lambda\psi_\Lambda) | \phi_0 \rangle + \langle \phi_0 | G_V^A(\rho) (\bar{\psi}\boldsymbol{\gamma}_\mu\psi) (\bar{\psi}_\Lambda\boldsymbol{\gamma}^\mu\psi_\Lambda) | \phi_0 \rangle \right\}. \quad (8)$$

Here $|\phi_0\rangle$ denotes the (hypernuclear) ground state. E_{free}^A is the contribution to the energy from the free relativistic hyperon including its rest mass M_Λ . The interaction term E_{int}^A includes density-dependent hyperon-nucleon vector (G_V^A) and scalar (G_S^A) couplings. They include mean-field contributions from in-medium changes of the quark condensates (identified with superscript (0)), and from in-medium pionic fluctuations governed by two-pion exchange processes (with superscript (π)):

$$G_i^A(\rho) = G_i^{A(0)} + G_i^{A(\pi)}(\rho) \quad \text{with} \quad i = S, V. \quad (9)$$

Minimization of the ground-state energy leads to coupled relativistic Kohn-Sham equations for the core nucleons and the single Λ -hyperon. Using the notation of Ref. [10], they read:

$$[-i\boldsymbol{\gamma} \cdot \boldsymbol{\nabla} + M_N + \gamma_0 (\Sigma_V + \Sigma_R + \tau_3 \Sigma_{TV}) + \Sigma_S + \tau_3 \Sigma_{TS}] \psi_k = \epsilon_k \psi_k \quad (10)$$

$$[-i\boldsymbol{\gamma} \cdot \boldsymbol{\nabla} + M_\Lambda + \gamma_0 \Sigma_V^A + \Sigma_S^A] \psi_\Lambda = \epsilon_\Lambda \psi_\Lambda, \quad (11)$$

where ψ_k and ψ_Λ denote the single-particle wave functions of the nucleon and the Λ , respectively. The single-particle Dirac equations are solved self-consistently in the “no-sea” approximation [19]. It is important to note that the rearrangement self-energy Σ_R [20] is confined to the nucleon sector because all the density dependent couplings are polynomials in k_f (and consequently in fractional powers of the baryon density through the relation $\rho = 2k_f^3/(3\pi^2)$), and there is no hyperon Fermi sea. The Λ self-energies read

$$\Sigma_V^A = G_V^A(\rho) \rho, \quad \Sigma_S^A = G_S^A(\rho) \rho_S, \quad (12)$$

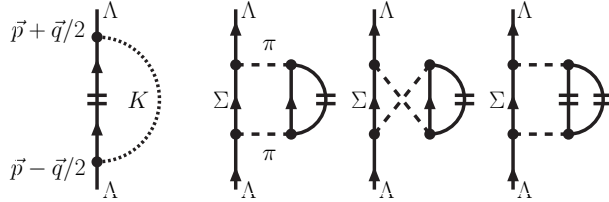
expressed in terms of the nuclear baryon and scalar densities, ρ and ρ_S .

In the following sections we analyze separately the different contributions to the density-dependent Λ -nuclear couplings $G_i^A(\rho)$, arising from the kaon- and two-pion-exchange induced Λ -nucleus potential, the condensate background mean-fields, and the pionic Λ -nucleus spin-orbit interaction.

2.2 Kaon- and two-pion exchange induced mean-field

The density-dependent self-energy of a zero-momentum Λ -hyperon in isospin-symmetric nuclear matter has been calculated in Ref. [17] at two-loop order in the energy density. This calculation systematically includes kaon-exchange Fock terms (first diagram in Fig. 3), and two-pion exchange with a Σ -hyperon and including Pauli blocking effects in intermediate states.

Fig. 3. One-kaon exchange Fock diagram and two-pion exchange Hartree diagrams with a Σ -hyperon in intermediate states. The horizontal double-lines represent the filled Fermi sea of nucleons in the in-medium propagator: $(\gamma \cdot p - M_N)[i(p^2 - M_N^2 + i\epsilon)^{-1} - 2\pi\delta(p^2 - M_N^2)\theta(p_0)\theta(k_f - |\mathbf{p}|)]$ [17].



The self-energy is translated into a mean field Λ nuclear potential $U_\Lambda(k_f)$. A cutoff scale $\bar{\Lambda} \simeq 700$ MeV (or equivalently, a contact term) represents short-distance (high momentum) dynamics not resolved at scales characteristic for the nucleon Fermi momentum. The value of $\bar{\Lambda}$ is adjusted to reproduce the empirical depth of the Λ nuclear central potential.

Following the procedure outlined in Appendix A of Ref. [10], we determine the equivalent density dependent Λ point coupling vertices $G_S^{A(\pi)}(\rho)$ and $G_V^{A(\pi)}(\rho)$. For the nucleon sector of the energy density functional the parameter set FKVW [10] is used. In Fig. 4 (case *a*) the Λ single-particle energy levels are plotted for the closed core of 16 nucleons ($8n + 8p$) plus a single hyperon (^{17}O). At this stage of the calculation the p -shell spin-orbit partners are practically degenerate, and the energies of the doublets are, by construction, close to their empirical values. Even the calculated energy of the s -state is realistic, although slightly too deep in comparison with data ($\epsilon_\Lambda^s = -12.42 \pm 0.05$ MeV for ^{16}O [5]).

Up to this point the in-medium chiral SU(3) dynamics (including K - and 2π -exchange) provides the necessary binding of the system, but no spin-orbit force. As it has already been shown in Ref. [10], the inclusion of derivative couplings does not remove the degeneracy of the spin-orbit partner states.

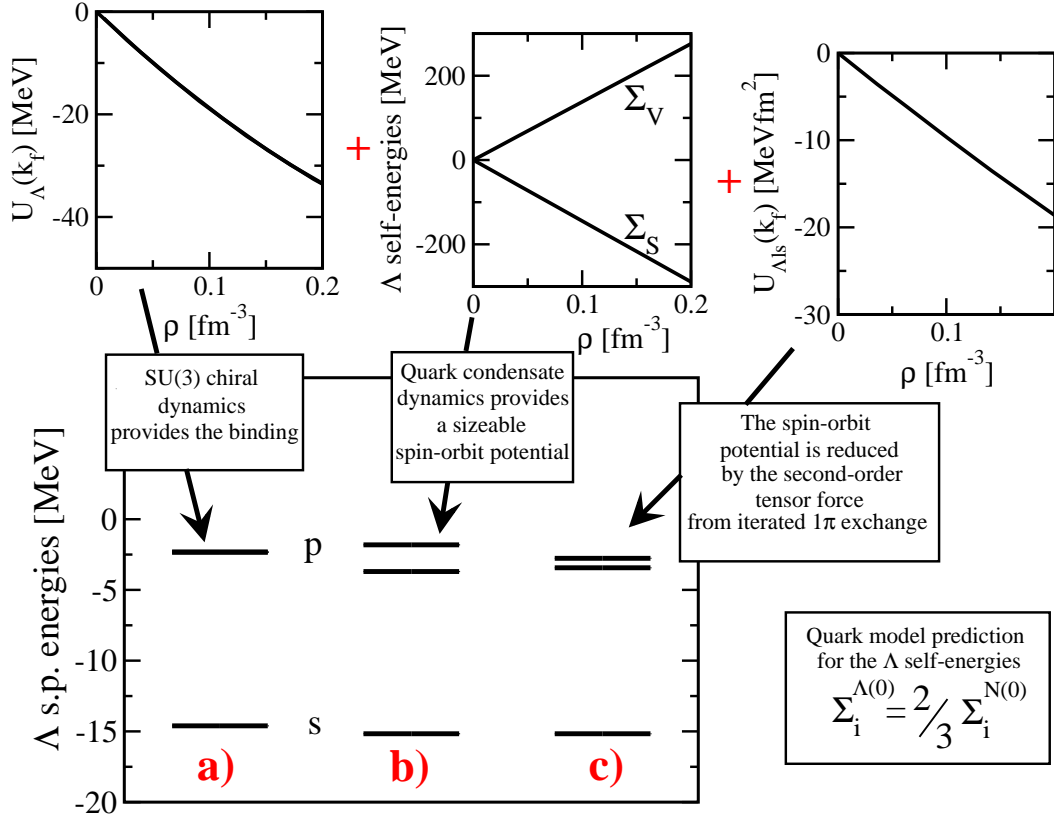


Fig. 4. Λ single-particle energy levels in ^{17}O : (a) the contribution of the single-particle potential with density-dependent coupling strengths determined in Ref. [17] by including chiral K - and 2π -exchange (see Sec. 2.2); (b) the spin-orbit effect from in-medium quark condensates has been included, with $\chi = 2/3$ corresponding to the simple quark-model prediction [21] (see Sec. 2.3); (c) the result of the additional compensating effect from the second-order ΛN tensor force with intermediate Σ (see Sec. 2.4)).

2.3 Background scalar and vector mean-fields

In contrast to the mean-field induced by kaon- and two-pion exchange, the condensate background Λ self-energies $\Sigma_V^{A(0)}$ and $\Sigma_S^{A(0)}$ produce a sizeable spin-orbit potential, analogous to the nucleon case [10]. Finite-density QCD sum rules predict moderate Lorentz scalar and vector self-energies for the Λ hyperon. Under some reasonable assumptions about the density dependence of certain four-quark condensates [22]², one expects a reduction of the corresponding couplings³

$$G_{S,V}^{A(0)} = \chi G_{S,V}^{(0)}, \quad (13)$$

by a factor χ , where $G_V^{(0)}$ and $G_S^{(0)}$ are the vector and the scalar couplings to nucleons arising from in-medium changes of the quark condensates, $\langle \bar{q}q \rangle$ and $\langle q^\dagger q \rangle$. The values of $G_V^{(0)}$ and $G_S^{(0)}$ have been determined by fitting to ground-state properties of finite nuclei [10], and found to be in good agreement with leading-order QCD sum rules estimates [11].

² While $\Sigma_V^{A(0)}$ is rather insensitive to the details of the calculation, $\Sigma_S^{A(0)}$ can only attain realistic values if the four-quark condensate $\langle \bar{q}q \rangle_{\rho_N}^2$ depends weakly on the nucleon density, and the four-quark condensate $\langle \bar{q}q \rangle_{\rho_N} \langle \bar{s}s \rangle_{\rho_N}$ has a strong density-dependence [22].

³ For simplicity the same reduction factor χ is used both for the scalar and vector self-energies. In general one could use two parameters (χ_S and χ_V), but the difference can be easily absorbed by the cut-off $\bar{\Lambda}$.

In Fig. 4 (case *b*) we plot the Λ single-particle energy levels calculated with the inclusion of these scalar and vector mean-fields, using the quark model prediction for the reduction parameter $\chi = 2/3$ [21]. In this case the p -shell spin-orbit partners are no longer degenerate. The calculated spin-orbit splitting is of the order of ~ 2 MeV. However, the choice $\chi = 2/3$ is a rather simplistic estimate. A detailed QCD sum rule analysis suggests a reduction to $\chi \sim 0.4 - 0.5$ [11,17,22], and to even smaller values if corrections from in-medium condensates of higher dimensions are taken into account. We note that the Λ -nuclear spin-orbit force is evidently still far too strong at this level, just as in the phenomenological relativistic "sigma-omega" mean-field models.

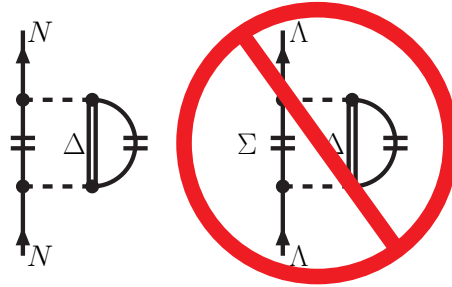
2.4 Λ -nuclear spin-orbit interaction from chiral $SU(3)$ two-pion exchange

The Λ -nucleus spin-orbit interaction generated by the in-medium two-pion exchange ΛN interaction has been evaluated in Ref. [17]. In the spin-dependent part of the self-energy of a Λ hyperon scattering in slightly inhomogeneous nuclear matter from initial momentum $\mathbf{p} - \mathbf{q}/2$ to final momentum $\mathbf{p} + \mathbf{q}/2$, one identifies the spin-orbit term $\Sigma_{ls}^{\Lambda}(k_f) = \frac{i}{2} U_{ls}^{\Lambda}(k_f) \boldsymbol{\sigma} \cdot (\mathbf{q} \times \mathbf{p})$. It depends only on known $SU(3)$ axial-vector coupling constants and on the mass difference between the Λ and Σ . The relevant momentum space loop integral is finite, and hence model independent in the sense that no regularizing cutoff is required. The result,

$$U_{ls}^{\Lambda}(k_f^{(0)}) \simeq -15 \text{ MeV fm}^2 \quad \text{at} \quad k_f^{(0)} \simeq 1.36 \text{ fm}^{-1},$$

has a sign *opposite* to the standard nuclear spin-orbit interaction⁴. This term evidently tends to largely cancel the spin-orbit potential generated by the scalar and vector background mean-fields. It is important to note that such a "wrong-sign" spin-orbit interaction (generated by the second-order tensor force from iterated pion exchange) exists also for nucleons [24]. However, this effect is compensated to a large extent by the three-body spin-orbit force involving virtual $\Delta(1232)$ -isobar excitations [25] (see Fig. 5), so that the spin-orbit interaction from the strong scalar and vector mean-fields prevails. For a Λ -hyperon, on the other hand, the analogous three-body effect does not exist, and the cancellation is now between spin-orbit terms from the (weaker) background mean-fields and the in-medium second-order tensor force from iterated pion-exchange with intermediate Σ . The small $\Sigma - \Lambda$ mass splitting, $M_{\Sigma} - M_{\Lambda} = 77.5$ MeV, plays a prominent role in this mechanism.

Fig. 5. Three-body diagram of two-pion exchange with virtual $\Delta(1232)$ -isobar excitation (left). For a nucleon it generates a sizeable three-body spin-orbit force of the "right sign". The horizontal double-line denotes the filled Fermi sea of nucleons. The analogous diagram does not exist for a Λ -hyperon (right), simply because replacing the external nucleon by a Λ -hyperon introduces as the intermediate state on the open baryon line a Σ -hyperon, for which there is no filled Fermi sea.



In order to estimate the impact of this genuine "wrong-sign" Λ -nuclear spin-orbit term, we introduce

$$\Delta \mathcal{H}_{ls}^{\Lambda} = -i \frac{U_{ls}^{\Lambda}(k_f^{(0)})}{2r} \frac{df(r)}{dr} \boldsymbol{\sigma} \cdot (\mathbf{r} \times \nabla), \quad (14)$$

⁴ Recall that nuclear Skyrme phenomenology gives $U_{ls}^N(k_f^{(0)}) = 3W_0\rho_0/2 \simeq 30 \text{ MeV fm}^2$ for the strength of the nucleon spin-orbit potential [23].

with the form-factor determined by the normalized nuclear density profile $f(r) = \rho(r)/\rho(r=0)$. The corrections to the Λ single particle energies ϵ_Λ are then evaluated in first-order perturbation theory:

$$\epsilon'_\Lambda = \epsilon_\Lambda + \langle \phi | \Delta \mathcal{H}_{ls}^A | \phi \rangle, \quad (15)$$

where $|\phi\rangle$ denotes the self-consistent solution of the system of Dirac single-baryon equations (10) and (11). In Fig. 4 (case *c*) one observes that the resulting p -shell single-particle energy levels, corrected according to Eq.(15), are close to being degenerate. The spin-orbit splitting is now strongly reduced, but still rather too large in comparison with empirical estimates. This could be a consequence of the possibly too large quark-model reduction factor $\chi = 2/3$. We note that within the range of values of χ compatible with QCD sum rules estimates, the empirical, almost vanishing spin-orbit splitting for the single- Λ states can indeed be obtained [18].

In Fig. 6 we plot the Λ spin-orbit spacing $\delta_\Lambda = \epsilon_\Lambda(1p_{1/2}^{-1}) - \epsilon_\Lambda(1p_{3/2}^{-1})$ as a function of the ratio χ between the background mean-fields for the Λ -hyperon and for the nucleon. The circles denote the spin-orbit splittings produced by the scalar and vector background fields alone. Even for unnaturally small values of χ , the splitting remains systematically too large in comparison with empirical estimates. Introducing the model-independent spin-orbit contribution from second-order pion exchange (Eq.(15)), these values are systematically reduced by about 1.3 MeV (triangles). For χ in the range 0.4 – 0.5 determined by the QCD sum rule analysis of Refs. [11,22], the small spin-orbit splitting is now reproduced in agreement with recent empirical values [5].

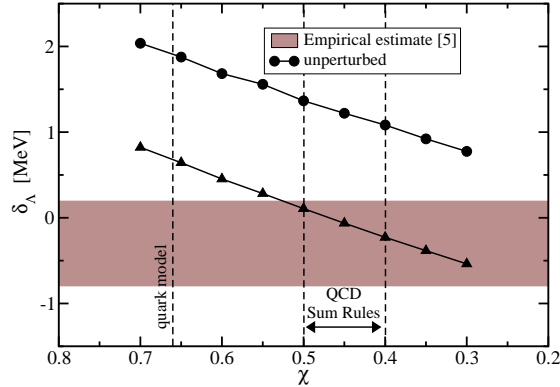


Fig. 6. Evolution of the spin-orbit splitting $\delta_\Lambda = \epsilon_\Lambda(1p_{1/2}^{-1}) - \epsilon_\Lambda(1p_{3/2}^{-1})$ in $^{17}_\Lambda\text{O}$, as a function of the ratio χ between the background self-energies of the Λ and nucleon. The dashed line at $\chi = 2/3$ denotes the simple quark-model value. Also indicated is the χ -interval allowed by the QCD sum rule analysis of Refs. [11,17,22]. Calculations with (without) the chiral SU(3) spin-orbit correction (Eq. (15)) are denoted by triangles (circles). The shaded area represents an estimate of δ_Λ ($-0.8 \text{ MeV} \leq \delta_\Lambda \leq 0.2 \text{ MeV}$) based on the measured energy difference $\Delta E(2_1^+ - 0_1^+)$ in $^{16}_\Lambda\text{O}$ [5].

3 Conclusions

The compensating mechanism for the spin-orbit interaction of the Λ -hyperon in nuclear matter, suggested in Ref. [17], successfully explains the very small spin-orbit splittings in finite Λ hypernuclei. We emphasize that this mechanism, driven by the second-order pion-exchange tensor force between Λ and nucleon, with intermediate Σ -states, is model-independent in the sense that it relies only on SU(3) chiral dynamics with empirically well determined constants. This intermediate-range effect (independent of any regularization procedure) counteracts short-distance spin-orbit forces. In ordinary nuclei, i.e. without hyperons, the corresponding effect is neutralized by three-body spin-orbit terms (induced by two-pion exchange with virtual Δ -isobar excitations). These terms are absent in hypernuclei. The theoretical framework based on in-medium chiral dynamics, described in this work, will be systematically applied to heavier hypernuclei.

Acknowledgements

I would like to thank my collaborators Dario Vretenar, Norbert Kaiser and Wolfram Weise, and acknowledge discussions with Avraham Gal and Achim Schwenk. This work was supported by INFN and MURST.

References

1. M. Danysz and J. Pniewski, *Phil. Mag.* **44** (1953) 348.
 2. R. E. Chrien and C. B. Dover, *Ann. Rev. Nucl. Part. Sci.* **39** (1989) 113.
 3. H. Bando, T. Motoba and J. Zofka, *Int. J. Mod. Phys. A* **5** (1990) 4021.
 4. D. J. Millener, C. B. Dover and A. Gal, *Phys. Rev. C* **38** (1988) 2700.
 5. O. Hashimoto and H. Tamura, *Prog. Part. Nucl. Phys.* **57** (2006) 564 and references therein.
 6. H. Kohri *et al.* [AGS-E929 Collaboration], *Phys. Rev. C* **65** (2002) 034607.
 7. N. Kaiser, S. Fritsch and W. Weise, *Nucl. Phys. A* **697** (2002) 255.
 8. S. Fritsch, N. Kaiser and W. Weise, *Nucl. Phys. A* **750** (2005) 259.
 9. P. Finelli, N. Kaiser, D. Vretenar and W. Weise, *Nucl. Phys. A* **735** (2004) 449.
 10. P. Finelli, N. Kaiser, D. Vretenar and W. Weise, *Nucl. Phys. A* **770** (2006) 1.
 11. T. D. Cohen, R. J. Furnstahl, D. K. Griegel and X. m. Jin, *Prog. Part. Nucl. Phys.* **35** (1995) 221.
 12. R. J. Furnstahl, J. J. Rusnak and B. D. Serot, *Nucl. Phys. A* **632** (1998) 607 [arXiv:nucl-th/9709064].
 13. R. J. Furnstahl and B. D. Serot, *Nucl. Phys. A* **673** (2000) 298 [arXiv:nucl-th/9912048].
 14. D. Vretenar, A. V. Afanasjev, G. A. Lalazissis and P. Ring, *Phys. Rep.* **409** (2005) 101.
 15. From relativistic mean-field phenomenology [12,13,14] it is well known that nucleons in the nuclear medium experience large scalar (Σ_S) and vector (Σ_V^0) self-energies. The nuclear spin-orbit potential naturally results from their coherent action (they nearly cancel in the central potential):

$$V_{ls} = \frac{1}{4\bar{M}^2} \left[\frac{1}{r} \frac{d}{dr} (\Sigma_V^0 - \Sigma_S) \right] \boldsymbol{\sigma} \cdot \mathbf{L} . \quad (16)$$
- with $\bar{M} = M - (1/2)(\Sigma_V^0 - \Sigma_S)$. On the other hand, in Ref. [26] it has been shown that contact terms at next-to-leading order (four terms with two derivatives, see Eq. (5) in Ref. [26]) also generate a large spin-orbit interaction
- $$iC_5(\boldsymbol{\sigma}_1 + \boldsymbol{\sigma}_2) \cdot (\mathbf{q} \times \mathbf{q}') , \quad (17)$$
- where the parameter C_5 is given by a linear combination of P -wave low-energy constants:
- $$C_5 = \frac{1}{16\pi} [2C(^3P_0) + 3C(^3P_1) - 5C(^3P_2)] . \quad (18)$$
- Apparently, it seems difficult to reconcile these two very different mechanisms of spin-orbit generation, but recently the necessary connection has been established [27]. Plohl *et al.* showed that, at the tree level, large Σ_S and Σ_V^0 are consistently generated by contact terms which occur precisely at next-to-leading order in the chiral expansion. This assertion appears to be rather robust even if one performs a more sophisticated many-body calculation (i.e. DBHF). Including condensate background fields does not spoil the consistency of in-medium chiral calculations based on the leading order πN Lagrangian.
16. R. Brockmann and W. Weise, *Phys. Lett. B* **69** (1977) 167; *Nucl. Phys. A* **355** (1981) 365.
 17. N. Kaiser and W. Weise, *Phys. Rev. C* **71** (2005) 015203.
 18. P. Finelli, N. Kaiser, D. Vretenar and W. Weise, submitted to *Phys. Lett. B*, arXiv:0707.3389 [nucl-th].
 19. B. D. Serot and J. D. Walecka, *Int. J. Mod. Phys. E* **6** (1997) 515; R. J. Furnstahl, *Lect. Notes Phys.* **641** (2004) 1.
 20. C. Fuchs, H. Lenske and H. H. Wolter, *Phys. Rev. C* **52** (1995) 3043.
 21. H. J. Pirner, *Phys. Lett. B* **85** (1979) 190; J. V. Noble, *Phys. Lett. B* **89** (1980) 325; B. K. Jennings, *Phys. Lett. B* **246** (1990) 325.
 22. X. m. Jin and R. J. Furnstahl, *Phys. Rev. C* **49** (1994) 1190.
 23. E. Chabanat, P. Bonche, P. Haensel, J. Meyer and R. Schaeffer, *Nucl. Phys. A* **635** (1998) 231.
 24. N. Kaiser, S. Fritsch and W. Weise, *Nucl. Phys. A* **724** (2003) 47 [arXiv:nucl-th/0212049].
 25. N. Kaiser, *Phys. Rev. C* **68** (2003) 054001 [arXiv:nucl-th/0312058].
 26. N. Kaiser, *Phys. Rev. C* **70** (2004) 034307 [arXiv:nucl-th/0407116].
 27. O. Plohl and C. Fuchs, *Phys. Rev. C* **74** (2006) 034325.